such as the Elsinore-Whittier fault system and the Newport-Inglewood fault zone, which strike subparallel to the San Andreas fault.

The strike-slip faults are typically well exposed at the surface, and earthquake hazards can be quantified through detailed studies of fault slip rates (*21*). In some areas, reverse or thrust faults of the Transverse Ranges are also exposed at the surface and can be studied in the same manner as strike-slip faults. In contrast, the Whittier Narrows earthquake indicates that a system of buried thrust faults presents additional potential earthquake hazards to the Los Angeles metropolitan area. These faults are at depths of 10 to 15 km within the crystalline basement and below a thick sedimentary rock section. The deformational history recorded in the sedimentary rocks commonly contains information about the offset and slip rate on these buried thrust faults (*22*). Furthermore, spatial distribution of small earthquakes (*3*) as well as secondary structural features within the sedimentary rocks may provide clues as to the size and segmentation of these buried thrust faults. Thus it may be possible to quantify the potential earthquake hazards from these buried thrust faults.

REFERENCES AND NOTES

1. Preliminary assessments of damage, made by the California Office of Emergency Services, are $252 million to private property and $106 million to local government facilities. These damage estimates are 50 times as large as the damage caused by the comparably sized 1984 Morgan Hill (M_L = 6.2) earthquake, which occurred in a much less densely populated area.
2. The main shock and its aftershock were recorded by the Caltech–U.S. Geological Survey southern California seismic network and the University of Southern California, Los Angeles, basin seismic network. In addition, several portable instruments were deployed to record aftershocks. The P and S wave arrival times at 80 of these seismic stations were inverted for hypocentral parameters, two crustal velocity models, and a set of station delay by the use of the VELEST computer algorithm (S. Roecker and W. L. Ellsworth, personal communication). The resultant velocity models are similar to those of (*3*). The first motion polarities that were recorded at these seismic stations were used to determine focal mechanisms for the main shock and 38 aftershocks. The orientations of the nodal planes were determined by the use of a grid-searching algorithm [P. Reasenberg and D. Oppenheimer, *U.S. Geol. Surv. Open-File Rep. 85-739* (1985), p. 46].
3. E. Hauksson, *Bull. Seismol. Soc. Am.* 77, 539 (1987).
4. L. M. Jones *et al.*, *ibid.* **76**, 1830 (1986).
5. The focal mechanisms of main shock and 38 magnitude 2.2 or higher aftershocks were inverted with the techniques of A. J. Michael [*J. Geophys. Res.* **89**, 1171 (1984)] to determine the deviatoric stress regime that best explains the data. Inverting the focal mechanisms for a stress field that is both uniform in space and constant in time results in a maximum compression axis that trends 163° (south-southeast) and plunges 6° and a most tensional stress axis that trends 50° (northeast) and plunges 66°. These orientations have a 95% confidence limit of ±20°. The magnitude of the intermediate deviatoric stress is near zero. The orientation of the maximum horizontal compressional axis (which in this case is also the maximum compressional axis) is rotated to the west from the maximum compressive stress that was determined for the western Los Angeles basin (*3*).
6. Geologic surface expression of the main shock appears to be limited to secondary nontectonic breaks that were caused by ground acceleration. Mapped faults in the vicinity of the epicenter and area of greatest cultural damage were field checked; no tectonic slippage was observed. Numerous ground cracks were observed along the base of the Puente Hills between Turnbull Canyon and Norwalk Boulevard. Although this area does contain the west-northwest extension of the Whittier fault, breakage was limited to slope failures that included extensional cracks along slope contours, minor landslides, and earthfalls. Surface cracks were also observed in relatively flat-lying areas of artificial fill (Worsham Creek oil field) and areas with shallow water table (Whittier Narrows golf course). Steep slopes in the area from the San Gabriel Mountains near Pasadena on the north to the Puente Hills south of Whittier suffered minor failures. Reporting of ground cracks near Whittier may partly reflect local hillside housing development and the extensive field search for surface rupture in that area.
7. J. H. Whitcomb, C. R. Allen, J. D. Garmany, J. A. Hileman, *Rev. Geophys. Space Phys.* **11**, 693 (1973).
8. W. L. Ellsworth *et al.*, *Science* **182**, 1127 (1973).
9. E. Hauksson and G. Saldivar, *Bull. Seismol. Soc. Am.* **76**, 1542 (1986).
10. Seismic moment is equal to the fault area × slip × rigidity. A seismic moment of 1.0×10^{25} dyne-cm gives a "moment magnitude" of M_w = 6.0, comparable to the local magnitude of M_L = 5.9 and the body-wave magnitude of m_b = 6.0.
11. A description of the technique and the dilatometer network is given in M. J. S. Johnston *et al.*, *Tectonophysics* **144**, 189 (1988).
12. T. H. Heaton and D. V. Helmberger, *Bull. Seismol. Soc. Am.* **69**, 1311 (1979). They calculated a seismic moment of 1.4×10^{26} dyne-cm for the 1971 San Fernando earthquake.
13. E. Etheredge and R. L. Porcella, *U.S. Geol. Surv. Open-File Rep. 87-616* (1987); M. Celebi *et al.*, *U.S. Geol. Surv. Open-File Rep. 87-621* (1987); A. F. Shakal *et al.*, *California Div. Mines Geol. Spec. Rep. OSMS 87-05* (1987).
14. J. C. Tinsley and T. E. Fumal, *U.S. Geol. Surv. Prof. Pap. 1360* (1985), p. 101.
15. C. F. Richter, *Elementary Seismology* (Freeman, San Francisco, 1958), p. 768.
16. Seismicity rates before the Whittier Narrows earthquake were calculated for earthquakes ($M_L \geq 2.5$) in the entire Los Angeles Basin, the Newport-Inglewood fault zone, and the northern section of the Elsinore fault zone. Aftershocks were removed from the data set by a computer algorithm (*17*). The statistical significance of the resulting rate fluctuations in these zones was assessed relative to a Poisson model of occurrence (*18*). The results indicate that there were no significant (n = 325; $P > 0.1$; where n is the number of events and P is the probability) rate fluctuations in the Los Angeles Basin during the 13.5-year interval before the main shock. In the North Elsinore fault zone, the seismicity rate decreased abruptly from approximately 6.0 earthquakes per year before 1983 to 2.6 earthquakes per year from 1983 to the time of the main shock. However, this decrease is not significant at the P = 0.1 level, in view of the low total number (57) of earthquakes that occurred there. Within the Newport-Inglewood fault zone, rate fluctuations were also not significant (n = 71; $P > 0.1$) during the 13.5-year interval. These results are consistent with those obtained for other moderate-sized earthquakes in California. Seismicity rates remained essentially constant during comparable intervals prior to the 1986 North Palm Springs (M_L = 5.6) earthquake, the 1984 Morgan Hill (M_L = 6.2) earthquake, and the 1979 Coyote Lake (M_L = 5.9) earthquake (*19*).
17. P. A. Reasenberg, *J. Geophys. Res.* **90**, 5479, 1985.
18. M. V. Matthews and P. A. Reasenberg, *Pure Appl. Geophys.*, in press.
19. P. A. Reasenberg and M. V. Matthews, *ibid.*, in press.
20. J. I. Ziony, Ed., *U.S. Geol. Surv. Prof. Pap. 1360* (1985).
21. K. E. Sieh, in *Earthquake Prediction: An International Review*, D. W. Simpson and P. G. Richards, Eds. (American Geophysical Union, Washington, DC., 1981), pp. 181–207.
22. T. Davis and K. Hayden, *Eos*, **68**, 1502 (abstr.) (1987).
23. C. W. Jennings, *Fault Map of California*, 1:750,000 scale, California Geologic Data Map Series, (California Division of Mines and Geology, Sacramento, 1975).

24. This research was supported by internal and external elements of the National Earthquake Hazards Reduction Program of the U.S. Geological Survey.

20 November 1987; accepted 4 February 1988

RNA as an RNA Polymerase: Net Elongation of an RNA Primer Catalyzed by the *Tetrahymena* Ribozyme

MICHAEL D. BEEN* AND THOMAS R. CECH

A catalytic RNA (ribozyme) derived from an intervening sequence (IVS) RNA of *Tetrahymena thermophila* will catalyze an RNA polymerization reaction in which pentacytidylic acid (C_5) is extended by the successive addition of mononucleotides derived from a guanylyl-(3′,5′)-nucleotide (GpN). Cytidines or uridines are added to C_5 to generate chain lengths of 10 to 11 nucleotides, with longer products being generated at greatly reduced efficiency. The reaction is analogous to that catalyzed by a replicase with C_5 acting as the primer, GpNs as the nucleoside triphosphates, and a sequence in the ribozyme providing a template. The demonstration that an RNA enzyme can catalyze net elongation of an RNA primer supports theories of prebiotic RNA self-replication.

SELF-SPLICING OF THE *Tetrahymena thermophila* precursor ribosomal RNA is mediated by the intervening sequence (IVS) portion of the RNA molecule. Splicing proceeds by two transesterification (phosphoester transfer) reactions. The first, attack by guanosine at the 5′ splice site, generates a 5′ exon with a free 3′ OH

Department of Chemistry and Biochemistry, University of Colorado, Boulder, CO 80309.

*Present address: Department of Biochemistry, Duke University Medical Center, Durham, NC 27710.

group. The second reaction, attack by the 3′ OH of the 5′ exon at the 3′ splice site, generates ligated exons and excised IVS containing the non-encoded G covalently bound to its 5′ end (*1*).

Portions of the excised IVS RNA act as enzymes (ribozymes), catalyzing reactions on exogenous RNA molecules with multiple turnover. These reactions occur by transesterification and are intermolecular versions of the two steps of self-splicing (*2–6*). One of these reactions bears a fundamental similarity to that catalyzed by RNA polymerase (*2, 7*). The L − 19 IVS RNA (linear IVS RNA missing 19 nucleotides from the 5′ end) catalyzes the disproportionation of pentacytidylic acid (C_5) to both longer and shorter oligomers of cytidylic acid. (Disproportionation is a reaction of the type $2\ C_5 \rightarrow C_4 + C_6$.) Although higher molecular weight RNA is produced, there is no change in the average molecular weight of the RNA in the population. The reaction mechanism involves a covalent intermediate that is a "charged" form of the ribozyme, with cytidylic acid transiently bound to the 3′ terminal guanosine (G^{414}) of the IVS. This form of the polymerase reaction requires that the growing chain dissociate from the ribozyme after each round of mononucleotide addition in order that the ribozyme be recharged. Upon being rebound and depending on whether the ribozyme is charged or uncharged, the oligonucleotide can be either elongated further or cleaved.

Recently, Kay and Inoue (*5*) have shown that a portion of the IVS RNA, missing short sequences at both the 5′ and 3′ end, can catalyze a transesterification reaction between dinucleotides. With the substrates CpU and GpN (N representing C, U, A, or G), the nucleoside monophosphate, pN, is transferred to the 3′ end of CpU; the reaction is the equivalent of the second step in splicing. This suggested a possible alternative to the disproportionation reaction described above. Rather than requiring the ribozyme to be recharged by the addition of pC to the 3′ end of the IVS for each cycle of nucleotide addition, it seemed possible that free GpC, or the other GpNs, could substitute for the G^{414}pC at the 3′ end of the charged ribozyme. An oligonucleotide would then be elongated at the expense of cleavage of substrate dinucleotides instead of other oligonucleotide products.

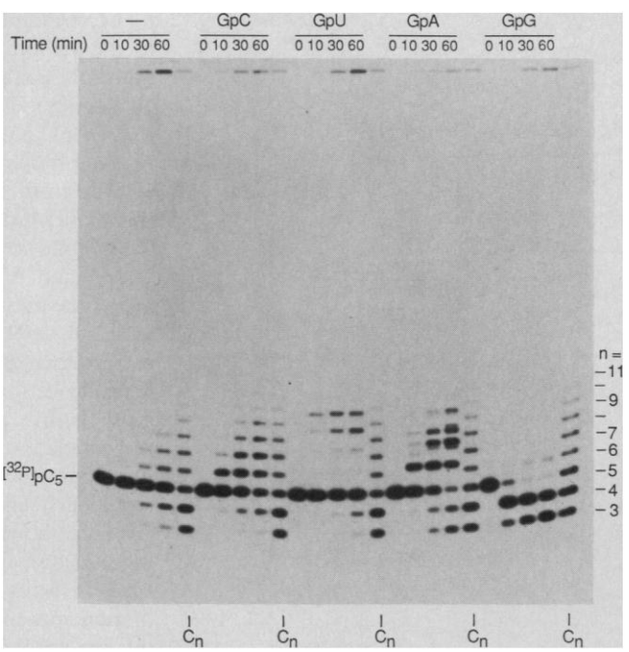

Fig. 1. Extension of pC_5 in the presence of L − 21 Sca I RNA and GpN. Each reaction contained 5 μ*M* [^{32}P]pC_5, 50 m*M* tris-HCl (*p*H 7.5), 50 m*M* $MgCl_2$, 0 or 0.5 m*M* GpN as indicated, and 1 μ*M* L − 21 Sca I RNA. The final volume was 10 μl and incubation was at 42°C. After addition of the L − 21 Sca I RNA, 2-μl portions were removed and mixed with 8 μl of formamide containing 25 m*M* EDTA and 0.03% xylene cyanol at the indicated times. A 4-μl portion of each sample was then fractionated on a 20% polyacrylamide gel containing 50% (w/v) urea. An autoradiogram of the gel is shown. Lanes marked C_n contain an oligo(C) ladder generated by L − 19 IVS RNA–catalyzed disproportionation of pC_5; L − 19 IVS RNA replaced the L − 21 Sca I RNA, and no dinucleotide was included, otherwise the reaction conditions were the same as above, and the reaction was terminated after 15 minutes. Near the top of the gel is a labeled band that increases in intensity with time and that migrates at a position expected for the L − 21 Sca I RNA. The major product at that position has been sequenced. On the basis of the sequence and results from additional studies, it was concluded that the major product is generated by pC_5 attack at the phosphate that follows G^{22} in the linear form of the L − 21 Sca I RNA. Preparation of the L − 21 Sca I RNA was as follows. The plasmid pT7L-21 (*8, 20*) contains a synthetic phage T7 promoter inserted such that RNA synthesis starts at position 22 in the IVS. The plasmid was cleaved with the restriction endonuclease Sca I, such that the T7 RNA polymerase runoff transcript ends at position 409, five bases before the 3′ splice site. The L − 21 Sca I RNA was purified by denaturing polyacrylamide gel electrophoresis and Sephadex G25 column chromatography. A small amount of 5′ end-labeled pC_5 was mixed with a known concentration of unlabeled C_5; the stated concentration of [^{32}P]pC_5 therefore represents the sum of pC_5 plus C_5.

The ribozyme used for the following experiments, "L − 21 Sca I RNA," has a 5′ end corresponding to position 22 in the IVS and a 3′ end at position 409, five bases before the 3′ splice site. It was made by transcription of Sca I–cut pT7L-21 DNA with T7 RNA polymerase (*8*). L − 21 Sca I RNA (1 μ*M*) was incubated with 5 μ*M* [^{32}P]pC_5 in 50 m*M* tris-HCl (*p*H 7.5), and 50 m*M* $MgCl_2$ at 42°C, and the products were analyzed by polyacrylamide gel electrophoresis and autoradiography (Fig. 1). In the absence of GpN, an oligo(C) ladder was produced after 30 minutes, presumably the result of the residual disproportionation activity of the L − 21 Sca I RNA preparation (*9*). However, when 0.5 m*M* GpC was added to the reaction, the average size of the labeled oligonucleotide increased.

The oligonucleotides generated by reaction of GpC with L − 21 Sca I RNA comigrated with the oligo(C) ladder, whereas the products observed in the reactions of GpU and GpA had mobilities that were shifted relative to the oligo(C) ladder. The products of reactions with GpU and GpA were identified by direct sequencing (*10, 11*). The decanucleotide produced in the reaction with GpU had the sequence C_5U_4X, and the heptanucleotide produced in the reaction with GpA had the sequence C_5AX. Although the 3′ terminal nucleotide X was not identified, the electrophoretic mobility was consistent with its being a U for the product of the reaction with GpU and an A for the product of the reaction with GpA. Thus, the initial reactions can be described as $*pC_5 + GpN \rightarrow *pC_5pN + G$ and subsequent steps as $*pC_5pN_i + GpN \rightarrow *pC_5pN_{i+1} + G$, where N = A, C, or U, $i \geq 1$, and *p is the labeled phosphate.

In the presence of GpG very little extension of C_5 occurred under the conditions of the experiment described in Fig. 1. A band comigrating with C_6 was probably C_6-generated by the residual disproportionation activity. At lower concentrations of both enzyme and substrates, a small amount of a product that could be C_5G has been seen (*10*), but the major products appeared to be C_3 and C_4 as seen in Fig. 1. In the first step of the splicing reaction, trinucleotides ending in G will substitute for guanosine in attack at the 5′ splice site of the precursor RNA (*12*), so it is expected that the dinucleotides with a 3′ G_{OH} would have similar activity. Thus, it is not surprising that the L − 21 Sca I RNA catalyzes reactions of the type $*pC_5 + GpG \rightarrow *pC_4 + GpGpC$, generating ^{32}P-labeled C_4 and C_3. This reaction would be similar to the guanosine-dependent endonuclease activity described previously (*3*).

The effect of varying the dinucleotide

concentration was examined (Fig. 2). The rate of elongation increased with increasing concentrations of GpC. With increasing GpU concentrations the amount of product in the 10-minute reaction increased although the average size of the elongated product then decreased with increasing time of incubation. With both GpC and GpU, up to five bases were efficiently added to the C_5. With longer exposures of autoradiograms of a C-addition reaction, it was possible to see oligo(C) bands up to about 20 bases in length, but they represented a small fraction of the products. With GpA, two nucleotides were efficiently added although three or four nucleotides were added in lesser amounts. From the rate at which the C_5 was consumed it appeared that GpA was more reactive than either GpC or GpU (*13*).

What might place an upper limit on the size distribution of the products? One possibility is that there is a competing reaction that breaks down the products. In every reaction, products smaller than the primer are generated. Some C_4 and C_3 might be generated by the residual disproportionation activity of the L − 21 Sca I RNA. Another possibility is that a size constraint, imposed by the oligonucleotide binding site, limits the extent of elongation. Finally, because guanosine is generated in the reaction, it is possible that there is cleavage of oligonucleotide products by guanosine attack (*3*).

In accordance with the last possibility, the addition of guanosine to the reaction was found to decrease the average size of the oligonucleotides generated and increase the amount of C_3 and C_4 (*10*). The extent to which such a reverse reaction limits the size of the product was tested. Oligocytidylic acids of chain length 3, 4, 5, 7, 9, 10, and 11 were gel-purified and tested for extension in the presence of L − 21 Sca I RNA and GpC. No appreciable extension of C_3 was seen; C_4, C_5, and C_7 were extended to C_{10}; C_9 and C_{10} were extended to C_{11} and a trace amount of C_{12}; and C_{11} was extended to C_{12} with very low efficiency. Thus, generation of products larger than C_{11} was not facilitated by using longer primers. Only a small amount of guanosine would be generated by the limited amount of extension of C_{10} and C_{11}; thus the reverse reaction, attack by guanosine, does not appear to be the limiting factor. It was also observed that the larger oligonucleotides were cleaved to generate a ladder of products down to C_3. These smaller products were generated in the absence of added GpN, so the likely mechanism is attack by a 3′ terminal G, which is found on about 9% of the ribozyme (*9*), or hydrolysis catalyzed by the L − 21 Sca I RNA. [Such hydrolysis within oligopyrimidine sequences would be equivalent to site-specific hydrolysis at the 5′ splice site of the pre–ribosomal RNA (*14*) or at the circularization site of linear IVS RNA (*15*).] Thus cleavage by free guanosine cannot by itself explain the limited size distribution; other competing reactions appear to be important and a binding site size constraint remains a possibility.

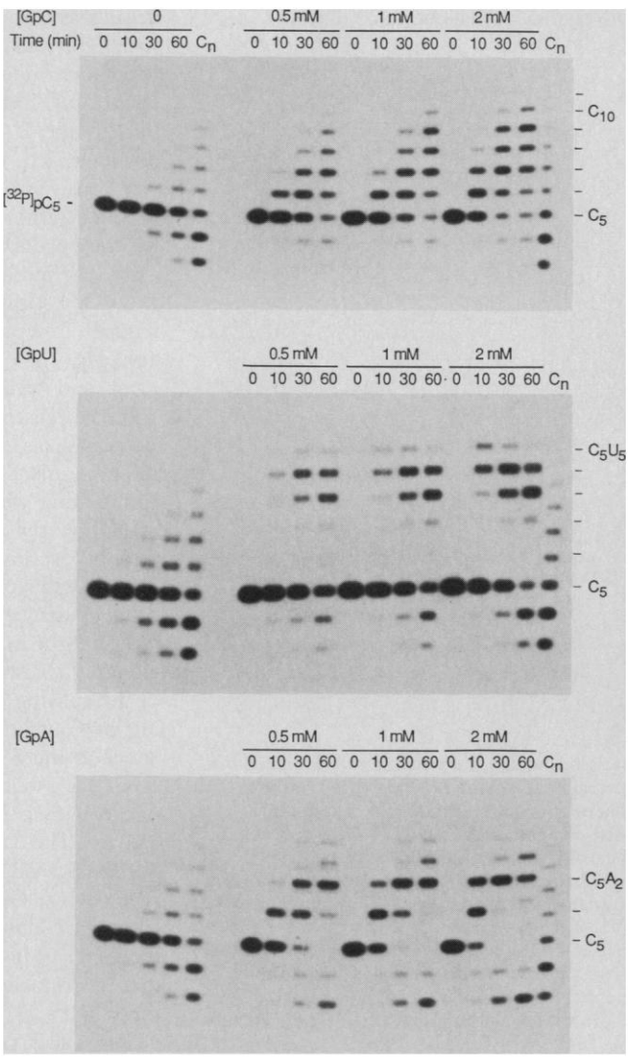

Fig. 2. Kinetics of polymerization with increasing concentrations of GpC, GpU, and GpA. Each reaction contained 50 m*M* tris-HCl (*p*H 7.5), 50 m*M* $MgCl_2$, 2 μ*M* [^{32}P]pC_5, 1 μ*M* L − 21 Sca I RNA, and no dinucleotide (0) or GpN at 0.5, 1, or 2 m*M*. Incubation was at 42°C; 2-μl portions were taken at 0, 10, 30, and 60 minutes and stopped as described in the legend to Fig. 1. Lanes marked C_n contain an oligo(C) ladder as described in the legend to Fig. 1.

Two models for the GpN-dependent polymerase reaction are presented in Fig. 3. In the distributive model (Fig. 3A), C_5 is bound in the 5′ exon binding site (GGAGGG at the 5′ end of the L − 21 Sca I RNA) (*2, 16, 17*) and the GpN is bound in the 3′ splice-site binding site (*5, 14, 15*). In a transesterification reaction that is equivalent to the second step in splicing (exon ligation), pN is transferred to the 3′ end of the C_5 and free G is produced. This is equivalent to the CpU plus GpN reaction described by Kay and Inoue (*5*), in which the production of G from the GpN was demonstrated. In this model further elongation requires that the oligonucleotide shift position, by dissociating and rebinding or by sliding, and guanosine must be released and replaced by a second GpN. If the distributive model is correct, then one would not expect template dependence for the added nucleotides, because the L − 21 Sca I RNA (and therefore the template region) does not extend 5′ to the binding site GGAGGG. In the processive model (Fig. 3B), the C_5 is positioned a few bases downstream of the 5′ exon binding site, at sequences that guide the circularization reaction (*18*), and successive rounds of mononucleotide addition can occur without the growing chain having to dissociate from the "template." Although the addition of C, U, and A means that addition is not strictly template-dependent, the greater extension by C and U compared to A is consistent with the elongation being template-influenced.

In the reaction described here, the *Tetrahymena* ribozyme has several replicase-like features. First, it requires a primer. Pentacytidylic acid was used in the experiments shown here and primers as short as C_4 are

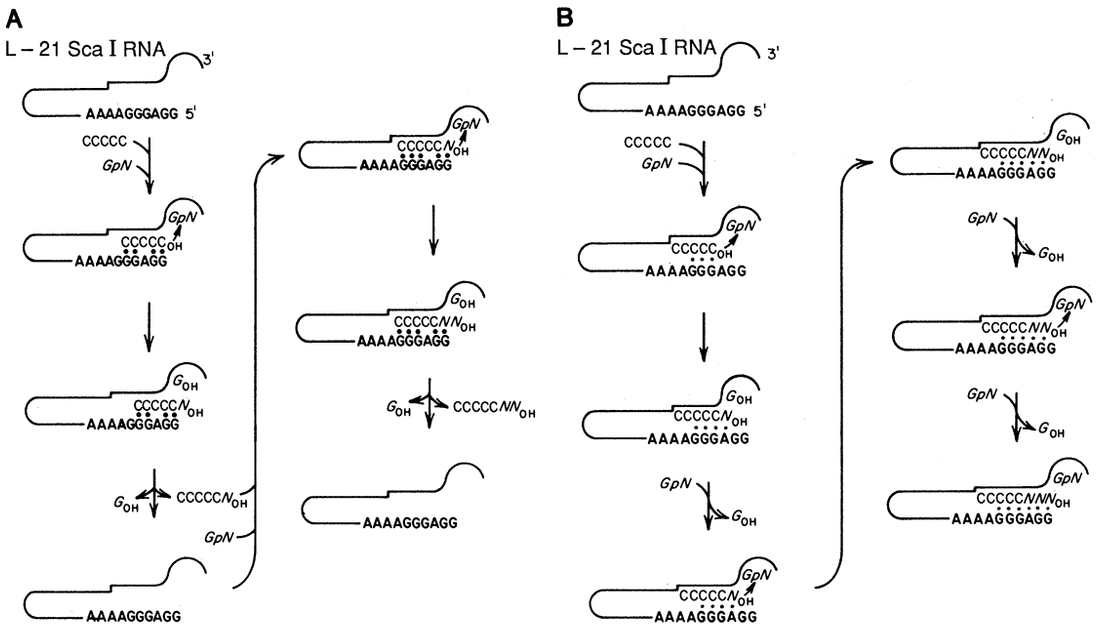

Fig. 3. Models for polymerization with GpNs as the source of the monomer units. (**A**) Distributive model. (**B**) Processive model. The L – 21 Sca I RNA, shown in boldface letters and solid line, begins with pppGGAGGG.

efficiently elongated. Second, like known replicases, it is a nucleotidyl transferase. Elongation of the primer occurs with the successive addition of mononucleotides and growth is in the 5′ to 3′ direction. The "activated mononucleotides" are provided as 5′ guanylyl derivatives rather than the 5′ triphosphates used in contemporary polymerase reactions. Finally, earlier studies have provided evidence for a required template-like structure. It has been shown that C_5 binds to the 5′ exon binding site in the IVS (*16*) and that this binding site may be able to slide through the catalytic center of the ribozyme in a template-like manner (*18*). Thus it seems possible that a form of the ribozyme missing its internal binding site might be able to track along an exogenous template.

Hypothesized mechanisms for RNA-catalyzed RNA replication and implications for early stages in the evolution of self-replicating systems have been described (*7, 19*). The demonstration of net elongation of an RNA primer by an RNA enzyme helps establish the principle that RNA might be capable of efficient self-replication. At the same time, the present work has revealed significant obstacles to a ribozyme derived from the *Tetrahymena* self-splicing IVS RNA to act as an efficient replicase. First, it appears difficult to incorporate G into a growing chain, because the guanosine donor (GpG) cleaves the chain. This problem may be intrinsic to the *Tetrahymena* IVS if the same binding site that binds free guanosine also binds the 3′ splice site and 3′ splice-site equivalents such as GpN (*5, 14, 15*). In a ribozyme replicase, this problem might be solved if the mononucleotides were donated not by GpN but by XpN, where X is a fifth nucleotide or some other group (for example, pyrophosphate). A second obstacle is the apparent template independence of nucleotide addition. The reaction clearly does not have the template dependence seen with contemporary DNA and RNA polymerases, where the incoming base must pair with the next position in the template as a prerequisite to efficient covalent bond formation. The lack of template dependence for the added nucleotide in the ribozyme reaction can be better interpreted after it is determined whether the reaction is distributive (Fig. 3A), processive (Fig. 3B), or some combination. In its present form, however, the polymerization reaction catalyzed by the *Tetrahymena* ribozyme seems better characterized as template-influenced rather than template-dependent. A third obstacle is the limited extent of chain elongation. It is possible that this problem might be solved by a ribozyme replicase that utilized an external template.

REFERENCES AND NOTES

1. T. R. Cech and B. L. Bass, *Annu. Rev. Biochem.* **55**, 599 (1986); T. R. Cech, *Science* **236**, 1532 (1987).
2. A. J. Zaug and T. R. Cech, *Science* **231**, 470 (1986).
3. A. J. Zaug, M. D. Been, T. R. Cech, *Nature (London)* **324**, 429 (1986).
4. J. W. Szostak, *ibid.* **322**, 83 (1986).
5. P. S. Kay and T. Inoue, *ibid.* **327**, 343 (1987).
6. In addition, a shortened form of the IVS RNA acts as a phosphotransferase and an acid phosphatase [A. J. Zaug and T. R. Cech, *Biochemistry* **25**, 4478 (1986)], activities that involve the same active site used in the nucleotidyl transfer reactions (*2–5*) but do not have counterparts in the reactions of self-splicing.
7. T. R. Cech, *Proc. Natl. Acad. Sci. U.S.A.* **83**, 4360 (1986).
8. A. J. Zaug, C. Grosshans, T. R. Cech, in preparation.
9. The residual disproportionation activity is presumably due to a small portion of the L – 21 Sca I RNA having a 3′ terminal G instead of the 3′ terminal U expected from the DNA sequence. Transcription of truncated DNA templates by T7 RNA polymerase frequently leads to the incorporation of extra nucleotides beyond those specified by the template [P. Lowary, J. Sampson, J. Milligan, D. Groebe, O. C. Uhlenbeck, in *Structure and Dynamics of RNA*, P. H. van Knippenberg and C. W. Hilbers, Eds., NATO ASI Series A, vol. 110 (Plenum, New York, 1986), pp. 69–76; J. F. Milligan, D. R. Groebe, G. W. Witherell, O. C. Uhlenbeck, *Nucleic Acids Res.* **15**, 8783 (1987)]. When transcripts of Sca I–truncated pT7L-21 DNA are 3′ end-labeled with [^{32}P]pCp and RNA ligase, digested to completion with ribonuclease T2, and the nucleoside 3′-phosphate products analyzed by thin-layer chromatography, it is found that 9% of the labeled nucleotides are G (*8*). If there is no bias in labeling of different 3′ ends by RNA ligase, this result indicates that 9% of the L – 21 Sca I RNA has a 3′-terminal G. To compare the residual disproportionation activity of the L – 21 Sca I RNA with that of the L – 19 IVS RNA, note in Fig. 1 that the amount of reaction generated by the L – 21 Sca I RNA in 60 minutes is considerably less than that generated by the L – 19 IVS RNA in 15 minutes (lanes C_n).
10. M. D. Been and T. R. Cech, data not shown.
11. RNA sequencing of the 5′ end-labeled oligonucleotides was done by the method of H. Donis-Keller, A. M. Maxam, and W. Gilbert [*Nucleic Acids Res.* **4**, 2527 (1977)], with the use of ribonucleases PhyM, U2, and T1.
12. P. J. Grabowski, thesis, University of Colorado (1983).
13. It is of interest to compare these substrate sequences with sequences of equivalent positions in the precursor RNA. The sequence at the 3′ splice site is GpU, where G is the last base in the intron and U is the first base in the 3′ exon. In a reaction containing GpU, once the C_5 has been extended by the addition of U, the oligonucleotide and GpN would most closely resemble the normal sequences of the 5′ exon and the 3′ splice site, respectively.
14. T. Inoue, F. X. Sullivan, T. R. Cech, *J. Mol. Biol.* **189**, 143 (1986).
15. N. K. Tanner and T. R. Cech, *Biochemistry* **26**, 3330 (1987).
16. M. D. Been and T. R. Cech, *Cell* **47**, 207 (1986).
17. R. B. Waring, P. Towner, S. J. Minter, R. W. Davies, *Nature (London)* **321**, 133 (1986).
18. M. D. Been and T. R. Cech, *Cell* **50**, 951 (1987).
19. P. A. Sharp, *ibid.* **42**, 397 (1985); N. R. Pace and T. L. Marsh, *Origins Life* **16**, 97 (1985); L. E. Orgel, *J. Theor. Biol.* **123**, 127 (1986); A. M. Weiner, in

Molecular Biology of the Gene, J. D. Watson *et al.*, Eds. (Benjamin Cummings, Menlo Park, 1987), vol. 2, pp. 1098–1163.
20. The plasmid pT7L-21 was provided by C. Grosshans.
21. We thank A. Sirimarco for preparation of the manuscript. Supported by grants from the American Cancer Society (NP-374) and the National Institutes of Health (GM28039). T.R.C. is a research professor of the American Cancer Society.

14 December 1987; accepted 5 February 1988

Expression of the Murine Duchenne Muscular Dystrophy Gene in Muscle and Brain

JEFFREY S. CHAMBERLAIN,* JOEL A. PEARLMAN, DONNA M. MUZNY, RICHARD A. GIBBS, JOEL E. RANIER, ALICE A. REEVES, C. THOMAS CASKEY

Complementary DNA clones were isolated that represent the 5′ terminal 2.5 kilobases of the murine Duchenne muscular dystrophy (Dmd) messenger RNA (mRNA). Mouse Dmd mRNA was detectable in skeletal and cardiac muscle and at a level approximately 90 percent lower in brain. Dmd mRNA is also present, but at much lower than normal levels, in both the muscle and brain of three different strains of dystrophic *mdx* mice. The identification of Dmd mRNA in brain raises the possibility of a relation between human Duchenne muscular dystrophy (DMD) gene expression and the mental retardation found in some DMD males. These results also provide evidence that the *mdx* mutations are allelic variants of mouse *Dmd* gene mutations.

DUCHENNE MUSCULAR DYSTROPHY (DMD) is a severe, X-linked recessive degenerative muscle disease frequently associated in humans with varying degrees of mental retardation (*1*). Genomic and complementary DNA (cDNA) clones for portions of the DMD gene have recently been isolated from humans and mice, which allows increasingly accurate prenatal diagnosis and carrier detection of DMD (*2–5*). A complete understanding of the function of the DMD gene product and the mechanism by which an abnormal gene leads to muscular dystrophy can be facilitated by the study of mice as a model system. The mouse *Dmd* gene is expressed in both skeletal and cardiac muscle at levels similar to those found in humans (*5*). In addition, the mouse *Dmd* gene has recently been mapped to a region of the X chromosome similar to that of the mouse muscular dystrophy mutation, *mdx* (*6, 7*). These mapping data together with pathological studies of three independently derived *mdx* mutants suggest that the *mdx* mutations could be within the mouse *Dmd* gene (*8*). The availability of mouse models for DMD would provide an important system for the study of DMD and for the development of experimental therapeutic procedures for muscular dystrophy.

We have isolated several cDNA clones for the mouse *Dmd* gene from an adult ICR mouse muscle cDNA library prepared in λgt11 (*9*). Together these clones span 2.5 kb at the extreme 5′ end of the murine Dmd messenger RNA (mRNA). Aside from two apparently polymorphic base substitutions, these skeletal muscle clones are identical to the cardiac muscle cDNAs previously reported (*5*), confirming that the skeletal and cardiac muscle transcripts are not differentially spliced over this portion of the *Dmd* gene.

We examined the expression of the *Dmd* gene using RNA prepared from several tissues of ICR mice, *mdx* mice, and two new *mdx* isolates (designated 467 and 551) (*8*). Dmd mRNA was detected by Northern analysis at low levels in ICR skeletal and cardiac muscle, and at very low levels in brain, but was not detected in liver, kidney, or spleen (Fig. 1A) (*10*). When skeletal muscle from the three *mdx* mouse strains was examined, Dmd mRNA of apparently normal size was detected in each (Fig. 1A). However, Dmd mRNA was not detected via Northern analysis in the brain of any of the *mdx* strains (Fig. 1A) (*10*). To control for the amount of RNA loaded in each lane and to examine the integrity of the RNA samples, we rehybridized the Northern blot shown in Fig. 1 with muscle-specific [γ-phosphorylase kinase (γ-Phk) (*11*)] and ubiquitously expressed [hypoxanthine phosphoribosyltransferase (HPRT) (*12*)] cDNA probes (Fig. 1, B and C). The results indicated that the mutant muscle RNAs were underloaded and slightly less intact than the control RNA, whereas the *mdx* brain sample appeared slightly overloaded but as intact as the control brain RNA. This experiment demonstrated that approximately normal-sized Dmd mRNA was detectable in brain samples of ICR mice and in the muscle samples of all three mutant *mdx* mice. However, we could not be sure whether the weaker hybridization observed for the Dmd cDNA with muscle and brain RNAs from *mdx* mice reflected a reduction of Dmd mRNA levels or was due to differences in the quality and quantity of the RNA samples.

To explore the possibility of altered Dmd mRNA levels in the three strains of *mdx* mice, we elected to use the technique of ribonuclease A (RNase A) protection (*13*). This method is more sensitive than Northern analysis, is highly specific, and results in sharp bands due to protection from RNase A of a short, complementary RNA (cRNA) probe hybridized in solution to RNA. Figure 2A demonstrates that a cRNA probe transcribed from the 530-bp Hind III–Bgl II fragment at the 3′ end of the Dmd cDNA XD-1 (*9*) is protected from cleavage with a range of RNase A concentrations after hybridization with ICR skeletal muscle RNA (*14*). The probe is also protected by cardiac muscle RNA, to a lesser extent by brain RNA, but not by liver or transfer RNA (Fig. 2B) (*10*). Since an identical 530-bp fragment is protected from RNase A diges-

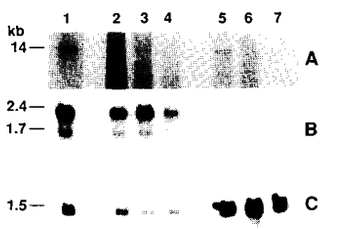

Fig. 1. Northern blot analysis of mouse RNAs. Samples (20 μg) of RNA from various tissues were isolated (*9*), separated by electrophoresis through 1% agarose/formaldehyde gels, transferred to GeneScreenPlus membranes (DuPont), and hybridized with cDNA probes essentially as described (*12, 20*). Autoradiograms from three successive hybridizations of the same blot with the indicated probes are shown. (**A**) Hybridization with Dmd cDNA XD-1 (*9*), (**B**) hybridization with mouse muscle γ-Phk cDNA Phk-2 (*11*), and (**C**) hybridization with mouse HPRT cDNA HPT5 (*12*). Lane 1, ICR skeletal muscle; lane 2, *mdx* skeletal muscle; lane 3, 467 skeletal muscle; lane 4, 551 skeletal muscle; lane 5, ICR brain; lane 6, *mdx* brain; and lane 7, ICR liver. Lane 1 in (A) and all lanes in (B) are from 24-hour exposures to film; the remaining lanes in (A) and those in (C) are from 72-hour exposures to film. Longer exposure of the blots in (B) reveals similar low levels of γ-Phk mRNA in ICR and *mdx* brain.

J. S. Chamberlain, J. A. Pearlman, D. M. Muzny, R. A. Gibbs, J. E. Ranier, A. A. Reeves, Institute for Molecular Genetics, Baylor College of Medicine, One Baylor Plaza, Houston, TX 77030.
C. T. Caskey, Institute for Molecular Genetics, Howard Hughes Medical Institute, Baylor College of Medicine, One Baylor Plaza, Houston, TX 77030.

*To whom correspondence should be addressed.